

Tribological Properties of Nano-dimensional Systems Containing Carbon Surfaces

A.V. Khomenko^{1,2,*}, N.V. Prodanov^{1,3,4,†}, K.P. Khomenko¹, D.S. Troshchenko¹

¹ Sumy State University, 2, Rimsky Korsakov Str., 40007 Sumy, Ukraine

² Peter Grünberg Institut-1, Forschungszentrum-Jülich, 52425 Jülich, Germany

³ Jülich Supercomputing Centre, Institute for Advanced Simulation, Forschungszentrum-Jülich, 52425 Jülich, Germany

⁴ Dept. of Materials Science and Engineering, Universität des Saarlandes, 66123 Saarbrücken, Germany

(Received 19 November 2013; revised manuscript received 25 November 2013; published online 06 April 2014)

We review tribological properties of boundary films of hydrocarbons and water confined between atomically smooth and rough surfaces. Both theory and experiment show that ultrathin film of liquid with thickness less than six molecular diameters restricted in small volumes is solid-like. Such a state is characterized by the decrease of mobility of molecules manifested in the increase of relaxation times and decrease of the diffusion coefficient. Additionally, quasidiscrete layers of molecules appear and in-plane ordering of the layers occurs. Atomic-scale roughness of the walls destroys the order of the molecules. We also describe experimental studies of friction of graphite at the atomic level. The experiments suggest a principal possibility of superlubricity for the tungsten tip of the friction force microscope sheared on the surface of graphite. A possible explanation of this phenomenon consists in the existence of the graphite nanoflake attached to the tip. However, reliable confirmation of this hypothesis is absent in the literature. We also review methods of the graphene preparation through exfoliation of a graphite sample and formation of defects in graphene as a result of its irradiation by different particles. We describe the experimental method of measurement of friction of metallic nanoparticles sliding on the surface of graphite. We consider basic advantages of this approach compared to the known methods and friction duality in these systems. The review indicates the necessity of further comprehensive theoretical study of friction of metallic nanoparticles adsorbed on atomically smooth surfaces.

Keywords: Boundary friction, Ultrathin lubricant film, Graphene, Adhesion, Exfoliation, Nanoparticle, Graphite, Molecular dynamics.

PACS numbers: 46.55.+d, 47.15.gm, 62.20.Qp, 64.60.-i, 68.35.Af, 68.37.Ps, 68.60.-p, 81.40.Pq

1. INTRODUCTION

Friction and wear are one of the oldest problems in physics which is of enormous practical importance [1-8]. Over many centuries, starting from ancient Egypt [2, 4] and up to the present days [5-7] and XXth century [9], understanding and control of these processes have attracted an increased attention. From the end of the XXth century, the fundamental investigations became concentrated on the phenomena occurring on very small spatial (and frequently time) scales. This has stimulated the appearance of a new direction, namely, nanotechnology [10, 11], which also includes the study of friction and wear of surfaces [12, 13]. Explanation of these processes at the atomic level is of a great importance from the fundamental point of view, since contact of surfaces in the majority of the cases is implemented on nanometer asperities [2, 3, 5, 6, and 14]. There is a suggestion that phenomena in macroscopic contacts can be represented as statistical combination of the behavior of separate nanosized contacts.

Individual nanocontact became an object of investigation of a new science – nanotribology. Its development recently is conditioned by the appearance of new experimental and theoretical methods [4]. The invention of the atomic [15] and frictional [16] force microscopy (AFM and FFM, respectively) allowed studying the tribological phenomena in dry nanocontacts. These techniques also

gave the possibility to manipulate nanosized structures and modify them [17-25]. Experimental investigation of microcontacts of the surfaces separated by a thin film of liquid is carried out using the surface force apparatus (SFA) [26-28]. Graphite and mica are often used as the materials for working surfaces in AFM, FFM and SFA, respectively, in the experiments for the purpose of decreasing the influence of random and uncontrolled factors. Layered structure of these materials gives the possibility to obtain atomically smooth surfaces. This fact as well as low friction coefficient of graphite [29] attracts an increased attention of researches to its nanotribological properties. On the other hand, the recent discovery of graphene [30] became the reason of an increased attention to its properties [31] including tribological ones [32-34]. Friction at the nanolevel of one of the hardest materials – diamond – also attracts a considerable attention [35].

Theoretical analysis plays a key role in revealing of the atomic reasons for friction. Phenomenological approaches, which are widely used for the interpretation of the experimental data and often applied in particular cases, mainly, allow obtaining a qualitative description only [36-42]. Molecular dynamics (MD) simulations of friction and wear at the atomic scale have significantly advanced understanding of the nature of nanotribological processes due to the fast growth of calculating ca-

* o.khomenko@mss.sumdu.edu.ua

† prodk@rambler.ru

capacity of computers [4, 43-47]. Below we consider the tribological properties of different nanosized systems discovered both experimentally and theoretically.

2. STRUCTURAL AND FRICTIONAL PROPERTIES OF THIN LIQUID FILMS

2.1 General properties

We have noted above that SFA allows to experimentally investigate the boundary lubrications [26, 27]. In particular, this device serves for the determination of surface forces acting on the atomically smooth surfaces of mica separated by molecules of liquid or gas. Using SFA one can measure shear (lateral) and normal forces (within the accuracy to ± 10 nN), shear rate and define distance between surfaces, their shape and real contact area. Optical interference of fringes of equal chromatic order is used for the measurements of the distance between the surfaces to within ± 0.1 nm.

Experiments show that properties of liquids confined in very small spaces qualitatively differ from those of the bulk liquids. Molecules of a liquid confined between atomically smooth surfaces are more ordered and form quasidiscrete layers [4, 26, 48]. In this case, the average local density of liquid experiences oscillations along the direction normal to the surfaces. Oscillations of density lead to oscillations of solvation force and are typical for simple nonpolar globular molecules (for example, octamethylcyclotetrasiloxane (OMCTS)), direct chain molecules (for example, *n*-hexadecane, *n*-C₁₆H₃₄) and even for chain molecules with sole methyl group in side flanking, for example, by 3-methylundecane C₁₂H₂₆ [49]. Investigations of solvation forces for longer and more branched molecules, for example, squalane compressed between mica surfaces have shown an absence of oscillations. Thus, branching of molecules leads to the destruction of the oscillatory behavior of the forces.

Boundary lubricant demonstrates two different responses to shear and change of the distance between friction surfaces. The first is a liquid-like, at which liquid flows under deformation. The second one is a solid-like and characterized by the yield strength of compressed liquid manifested in the absence of deformation before the critical value of shear stress leading to a stick-slip motion is achieved [4, 26, 48]. Sticks and slips alternate in the stick-slip motion. It is observed only for shear rates and temperatures less than some critical value.

Dynamics of a liquid on the interface and, especially, under limitation by solid surfaces “is considerably slowed down” [4, 26, 48-50]. Mobility of molecules in the films in a clumped state significantly reduces in comparison with volume liquids. This is reflected in the decrease of the diffusion coefficient and growth of viscosity and molecular relaxation times. “Effective” viscosity can reach values which are 10^5 times larger, and relaxation time can be 10^{10} times longer. Moreover, arrangement of molecules also influences the dynamics of compressed liquid. In particular, branched and long chain molecules are rearranged slower than the short ones.

MD simulations confirm the experimental results of the works [4, 7, 26, 47, 49-52]. Modeling of two plates separated by the Lennard-Jones (LD) liquids of the thickness not more than 6-10 molecular diameters shows that molecules between the surfaces form quasi-discrete la-

yers. Decrease in the diffusion coefficient and increase in the viscosity are also observed. Abrupt liquid-solid phase transition in the films of the thickness less than 6 molecular diameters exists in the case of atomically structured surfaces. Ordering of molecules in the directions perpendicular and parallel to the planes is typical for this transition.

We note that the horizontal order is absent for the unstructured (mathematically smooth) walls. Similarly to the experiments, strongly expressed quantized yield strengths were found for the structured surfaces which were not exhibited in the case of the unstructured plates. Calculations reliably denote the key influence of the atomic structure or “granularity” of real surfaces on the formation of the films with the same atomic sizes.

The authors of [49, 50] in the framework of large canonical ensemble studied the equilibrium properties of *n*-hexadecane and squalane limited by rigid golden walls. Oscillations of the density of compressed liquids related to the presence of layers are typical for straight and branched molecules (Fig. 1). Their amount is determined by the distance between the surfaces. A film of the *n*-hexadecane is characterized by greater in-plane ordering of layers and molecules (Fig. 2) compared to squalane, for which molecules of different layers mutually penetrate (Fig. 1).

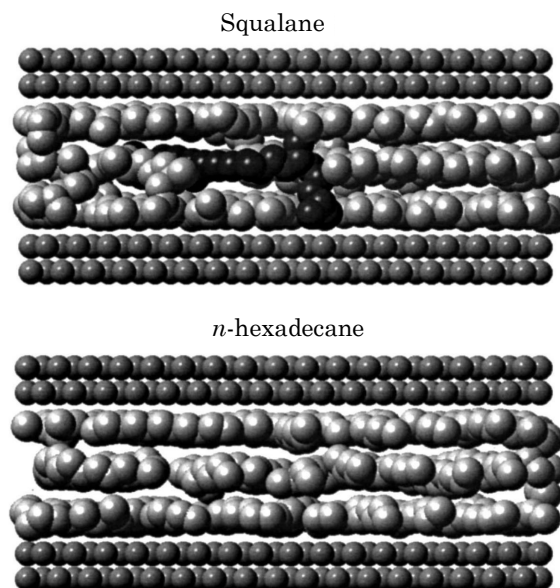


Fig. 1 – Lateral view of the squalane (top) and *n*-hexadecane (bottom) films showing molecular interlayer penetration (dark regions) in the squalane film. Small balls correspond to gold atoms. (Reprinted with permission from [49]. Copyright [1997], AIP Publishing LLC)

Dynamical processes in the boundary lubricant films including transition of a liquid to a solid-like state and stick-slip friction mode are studied by the MD method [53, 54]. According to [53], statistical surfaces induce a crystalline order of simple LD liquid. Stick-slip motion is a result of the periodic shear melting and film recrystallization. Uniform motion is realized at high velocities, when film does not have enough time for ordering. Thus, stick-slip motion is caused by the thermodynamic instability of the lubricant states and not by the dynamic instability as it was suggested earlier. It is shown in

the work [54] that at small distances between the walls the film consisting of linear chain molecules is amorphized, i.e. relaxation times rapidly increase. This is reflected in the decrease of the diffusion coefficient and in the response to shear. According to the experiments, viscosity depends on the shear rate by the power law.

Study of the influence of the atomic roughness or surface relief on the properties of boundary lubricants has gained an importance, too [51, 52, 55]. In particular, the authors of the work [51] investigated the friction of atomically smooth and atomically rough adhesive and repulsive surfaces of gold separated by the ultrathin film of hexadecane (Fig. 3).

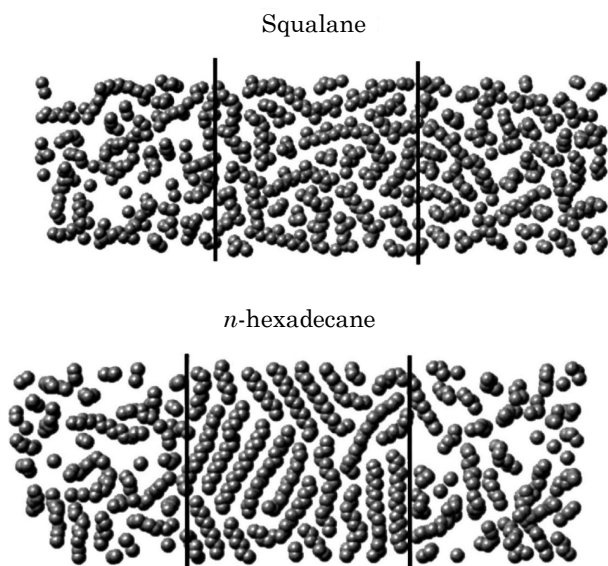


Fig. 2 – Top view of the equilibrium boundary layers of squalane (top) and *n*-hexadecane (bottom) which have 4 layers. Liquid is compressed in the region between the solid lines. We note an improved intra- and interplanar order in the film of *n*-hexadecane. (Reprinted with permission from [49]. Copyright [1997], AIP Publishing LLC)

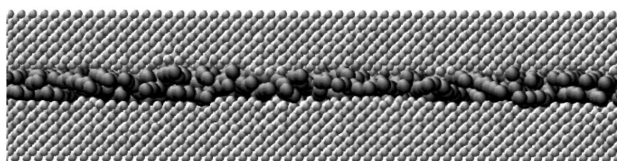


Fig. 3 – Atomically rough golden surfaces separated by molecules of hexadecane. (Reprinted with permission from [51]. Copyright [2004], American Chemical Society)

As seen from Fig. 4, layers are formed between smooth surfaces similarly to the experiments described above. According to the left and central columns of this figure, atomic relief destroys the vertical order irrespective of the type of interactions between molecules of the liquid with surfaces. Moreover, it is established [51] that atomic relief leads to the in-plane disorder (Fig. 5). Following [55], atomic roughness can considerably change adhesion forces between walls separated by molecules of the liquid. This is expressed in the drop of adhesion force as a result of the decrease in the real contact area.

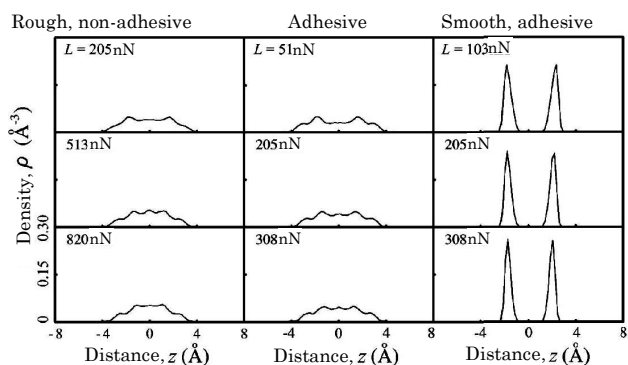


Fig. 4 – Segment density profiles of hexadecane in the direction of the axis normal to solid planes for different values of the applied load. The left column corresponds to the case of non-adhesive rough surfaces. Central and right columns correspond to the adhesive rough and adhesive smooth walls, respectively. (Reprinted with permission from [51]. Copyright [2004], American Chemical Society)

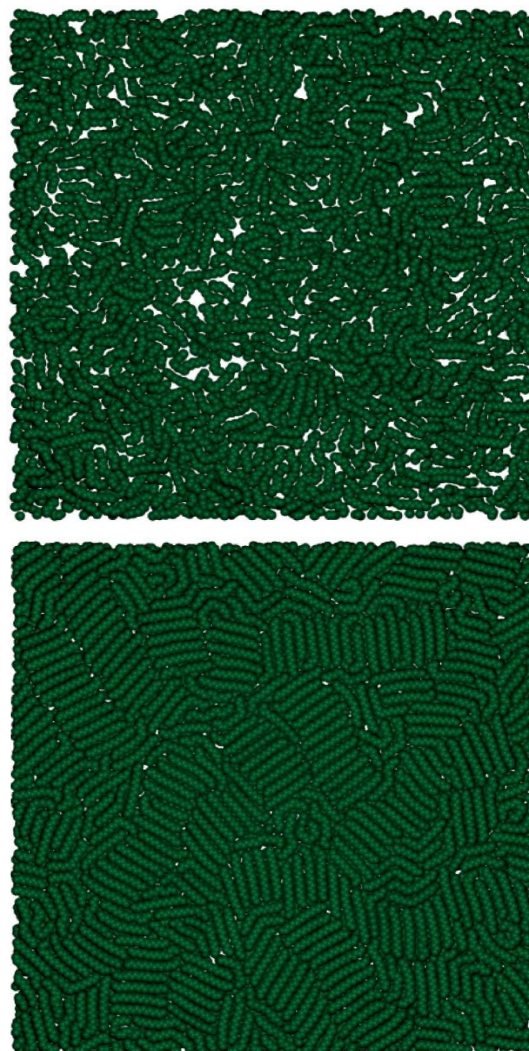


Fig. 5 – Top view of the arrangement of molecules in the contact region of solid surfaces. The upper figure corresponds to rough and the lower figure – to smooth walls. Adhesive interactions between molecules of hexadecane and gold atoms are realized in both cases. (Reprinted with permission from [51]. Copyright [2004], American Chemical Society)

Experimental [26, 48] and numerical [51] investigations of the friction force at different loads on surfaces have shown that Amontons macroscopic law (linear dependence of the friction force on the load) holds true. The influence of the atomic relief, type of interaction between molecules of liquids and surface and temperature changes on the mentioned dependence has quantitative but not qualitative character. The shear stresses can be changed with load in more complicated nonlinear way shown in Fig. 6 [26]. Its nature can be explained using the “cobblestone” model [6].

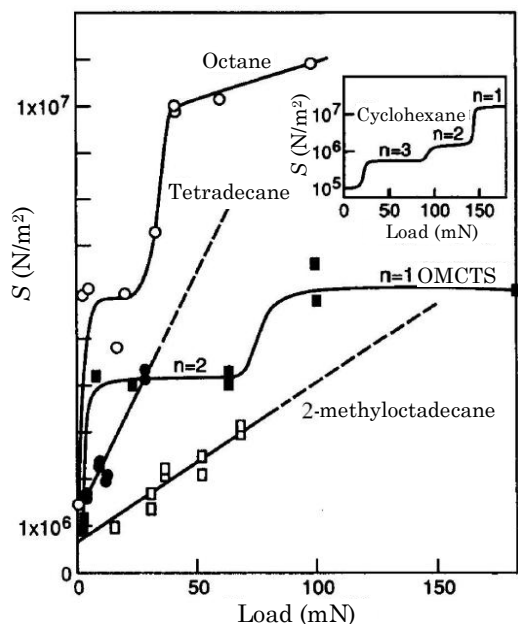


Fig. 6 – Shear stresses vs. the load in the stationary state for solid-like films. (Reprinted with permission from [26]. Copyright [1990], AIP Publishing LLC)

2.2 Properties of ultrathin water film

Up to this point, hydrocarbons have been considered. Behavior of other liquids under confinement is also of a great importance. In particular, the field of tribology studying biosystems, for example, mechanisms of lubrication in joints [8], has acquired popularity recently. It is known that systems, in which water plays the role of lubricant, are often found in the nature. By their characteristics they excel hydrocarbon lubricants, which are usually applied in practice. Many applied and fundamental investigations [8] are aimed at the formation of lubricants with properties of the natural ones.

To accomplish this purpose, it is necessary to understand the molecular properties of water, some of which characterize it as an unusual substance [28, 56]. Firstly, being a liquid with low molecular mass, water possesses uncharacteristic high temperatures of melting and boiling and specific evaporation heat. Secondly, the circumstance that molecules of ice are located farther from each other than in a liquid phase is reflected in the density maximum at 4°C and unusual phenomenon – solid water (ice) is lighter than liquid. Anomalous properties of water are the consequence of very strong and dependent on the orientation of intermolecular hydrogen bonds.

Presence of a monolayer of water molecules (of the

thickness of about 0.25 nm) between atomically smooth mica surfaces in SFA leads to the decrease in the friction force by more than one order of magnitude [4, 26, 28]. Friction coefficient accounts for 1-2 % of the value corresponding to the anomalously low friction of ice. A monolayer of water molecules decreases the friction force due to two circumstances: 1) “hydrophilicity” of the mica surface (mica is “moistened” by water); 2) strongly repulsive short-range hydration force between such surfaces in aqueous solutions, which effectively excludes the contribution of adhesion into the friction force. In this case, the first Amontons law holds for the friction force (it is proportional to the external load).

In the last years, properties of compressed water molecules were actively studied numerically by the MD method [52, 57-63]. The given works consider the equilibrium structural and dynamic characteristics of some models of water in the limiting pores of different forms.

Inhomogeneous distribution of water molecules (characterized by oscillating density profiles) is confirmed by TIP3P modeling of water molecules in hydrophobic cylindrical pores of different radii [57] and SPC/E molecules in a hydrophilic cylindrical cavity of high-silica glass [58, 59]. In the first case, the indistinctly expressed concentric layers are formed, and motion of molecules considerably slows down with the decrease in the cavity radius that follows from the measurement of the diffusion coefficient. In the second case, double layer is formed due to the water adsorption, and anomalous diffusion can be observed. Formation of a water layer around the hydrophilic quartz particles is shown by MD simulations of SPC/E water molecules confined in a gel of silicic acid [60]. Larger roughness of the quartz surface leads to the fact that formation of the second layer does not occur at both high and low densities. Consideration of water adsorption in the framework of the SPC/E model in attractive and repulsive slit-like pores [61] shows the formation of disordered (in-plane) layers for both types of pores at high densities of molecules. Moreover, the type of intermolecular interactions between water and surfaces can significantly influence the properties of a confined liquid. Modeling of SPC water in the interdomain region of multidomain BphC enzyme [62] also indicates the determining role of local surface curvature and hydrophobic property in the formation of the water structure and dynamics. Thus, according to numerical results, water in bounded spaces exhibits general properties of the compressed liquids.

3. FRICTION AND WEAR OF GRAPHITE SYSTEMS

3.1 Superlubricity phenomenon

Graphite surfaces, in particular, consisting of highly oriented pyrolytic form (HOPG), are widely used in the experiments of friction and wear at the atomic level [16-21, 64-67]. Atomic periodicity is the distinctive feature of the typical friction loop obtained using graphite scanning by the FFM tungsten probe [64, 68]. It implies that sliding is nonuniform, and atomic stick-slip motion takes place. It is difficult to explain this phenomenon, since a large amount of probe atoms are located in the contact area, and periodic behavior should not be displa-

yed. The first attempt to clarify the nature of the atomic periodicity consisted in the assumption that FFM probe pulls a graphite flake on the surface [64]. This approach was subsequently found to be untenable [68], since atomically periodic friction was also discovered for nonlaminar materials, in which a flake cannot be formed.

Dienwiebel et al. [5, 69] has developed a new design of the FFM with the lateral resolution up to 15 pN for the determination of friction of the tungsten probe on the graphite surface. A special friction sensor – Tribolover (Fig. 7) offers the feature of this FFM. In order to prevent the phenomenon “jump to contact” there, symmetrical springs with small elastic coefficient in two lateral directions combine with high rigidity in the normal direction. Tungsten probe is glued to Tribolover by silver epoxy resin and has an asperity of 50-60 μm out of the device. Shift of the Tribolover probe is detected by four glass-optical interferometers.

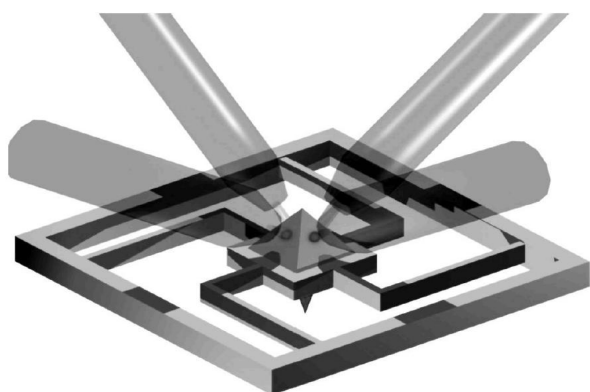


Fig. 7 – The model of silicon Tribolover. Four legs, placed symmetrically around central pyramid (which serves as mirror for interferometers), form a set of identically sensitive springs along the x - and y -directions. Tungsten probe is directed downwards [5]. (Reprinted with permission from [69], <http://prl.aps.org/abstract/PRL/v92/i12/e126101>. Copyright [2004] by the American Physical Society)

Design features of the probe with Tribolover allowed defining the friction force for the HOPG surface in any direction of sliding. Dependences of the friction force on the relative orientation of crystal lattices of the probe and sample are obtained (Fig. 8).

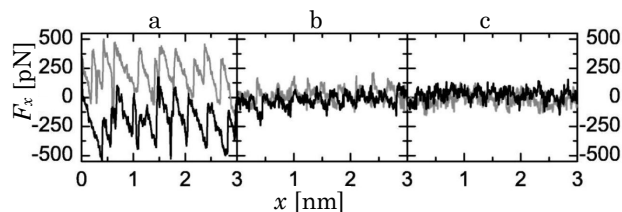


Fig. 8 – Friction loops (black color – direct, grey color – inverse scanning) determined along the direction of shear for the following angles of the probe/surface orientation: a) 60°, b) 72°, and c) 38°. Normal force accounts for 18 nN [5]. (Reprinted with permission from [69], <http://prl.aps.org/abstract/PRL/v92/i12/e126101>. Copyright [2004] by the American Physical Society)

Fig. 8a for lateral force shows that clearly expressed stick-slip motion of the atomic scale is realized. If the force exceeds some critical value, the probe advances a distance of the lattice constant of the graphite substrate. The area inside the friction loop determines the energy which is ir-

reversibly dissipated during sliding. The mentioned area, divided by a double loop width, corresponds to the average dissipative friction force of the probe which is equal to 203 ± 20 pN. Rotation of the graphite substrate by 12° clockwise around the axis, normal to the surface and parallel to the probe, at the same conditions which are shown in Fig. 8a leads to the decrease in the friction force more than by the order of magnitude to 15.2 ± 15 pN (Fig. 8b). If the sample is rotated in the opposite direction, friction force is reduced to almost zero value (Fig. 8c).

The presented results indicate the so-called superlubricity phenomenon consisting in the reduction of friction by orders of magnitude with changing the motion direction of the probe. The averaged friction force significantly depends on the direction of the graphite surface scanning. Two narrow angular peaks in Fig. 9 corresponding to high friction are separated by a wide range of angles corresponding to almost zero friction. The distance between the two friction maxima agrees with the 60-degree symmetry of the atomic planes of graphite. Based on this fact and good fit of the experimental results and numerical simulation within the framework of the modified Tomlinson model [70], one can conclude that super-lubricity is realized between the graphite sample and its flake attached to the probe. For two orientations, corresponding to the friction peaks, crystal lattices of the flake and substrate are perfectly oriented with each other, and they are incommensurable for intermediate angles.

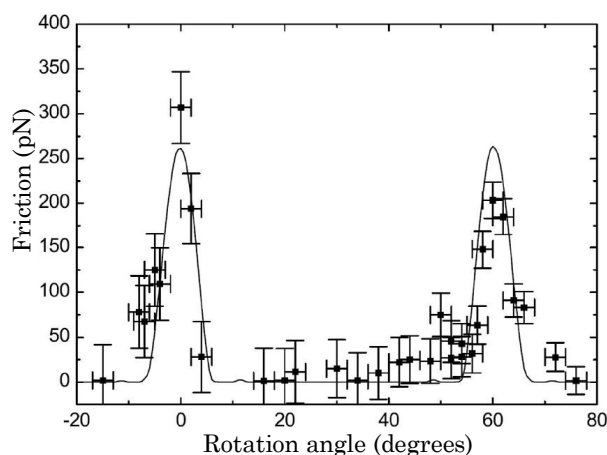


Fig. 9 – Dependence of the average friction force on the rotation angle of graphite around the axis normal to its surface. (Reprinted with permission from [69], <http://prl.aps.org/abstract/PRL/v92/i12/e126101>. Copyright [2004] by the American Physical Society)

However, the performed experiments do not contain reliable confirmation of the existence of a flake on the probe. Use of the transmission electron microscope (TEM) with high resolution did not give the possibility to conduct the necessary visualization of the FFM probe [5, 69]. Since experiments were carried out in open conditions, but not in a vacuum, the probe was covered by amorphous oxide layer. It has almost completely disappeared under the action of electron radiation during some minutes of TEM operation; and graphite flake (if it was present) was removed with amorphous layer. Moreover, according to [69], the experiments to obtain Fig. 9 are not reproducible. Thus, the investigations confirming attachment of a flake to the FFM probe and determining the conditions of its formation are required.

3.2 Micromechanical graphite cleavage

Along with the above described experimental results, one of the methods for producing atomically smooth surfaces is based on exfoliation of graphite [5, 17, 67, 69]. Understanding of the mechanisms underlying the given phenomenon is important both from the specified practical point of view and for the optimization of the micromechanical exfoliation, i.e. the method which helped to discover graphene (a layer of carbon atoms in the hexagonal close packed lattice) [30].

Theoretical investigations of the band structure and electronic characteristics of graphene have shown that it exhibits unusual electronic properties [71, 72]. Its experimental production in recent years allowed verifying the theoretical results, some of which were found to be true. In particular, charges in graphene represent massless Dirac fermions [73], and here Born-Oppenheimer approximation [74] is inapplicable and quantum Hall effect is observed at room temperature [75]. The listed anomalous properties make graphene to be a promising material for electronic engineering of the “post-silicon era” [71, 72]. Modern field-effect transistors, transparent conducting electrodes, sensors, energy converters and storage systems, photoanodes in photoelectrochemical cells, biocompatible materials, etc. can be produced based on graphene [76].

The absence of high-production method for producing graphene puts it on a par with new materials. In spite of the considerable progress in the field of epitaxial techniques [31], a complete growth cycle of one graphene layer is not still established. Micromechanical exfoliation, which is also called the “scotch-technology”, is the standard procedure for producing graphene [30, 71]. The given technique allows to divide graphite into individual atomic planes using adhesion tape. The majority of the researches still uses scotch-technology for the production of high-quality graphene [31, 77].

There exist other new effective techniques for producing graphene which are also based on exfoliation of graphite [78-80]. The method for producing graphene by dispersion and exfoliation of graphite in organic solvents, in particular, N-methylpyrrolidone is proposed [78]. The authors of the work [79] have developed the solvothermal method, when thermally expanded graphite is divided in highly-polar organic solvent under the ultrasonic action. Use of electrostatic forces for the specified purposes [80] is schematically shown in Fig. 10. A lithographic deposition of nanometer relief on the surface of HOPG disk with subsequent reactive ion etching is performed in this case (Fig. 10a). Structured HOPG disk acting as a template is placed into contact with Si / SiO₂ substrate. Electrical voltage is applied between HOPG and silicon and causes the appearance of attractive forces which act between graphite relief and silicon substrate (Fig. 10b). Removal of the HOPG template from the substrate in the vertical direction in electrostatic field is accompanied by exfoliation of graphite and attachment of graphene particles, which contain some layers, to the substrate (Fig. 10c). Small depth of screening in HOPG (less than 0.5 nm) indicates that electrostatic force influences only very external graphene planes during the cleavage cycle. This method combined with other nanolithographic approaches seems to be promising for producing large integral schemes based on graphene.

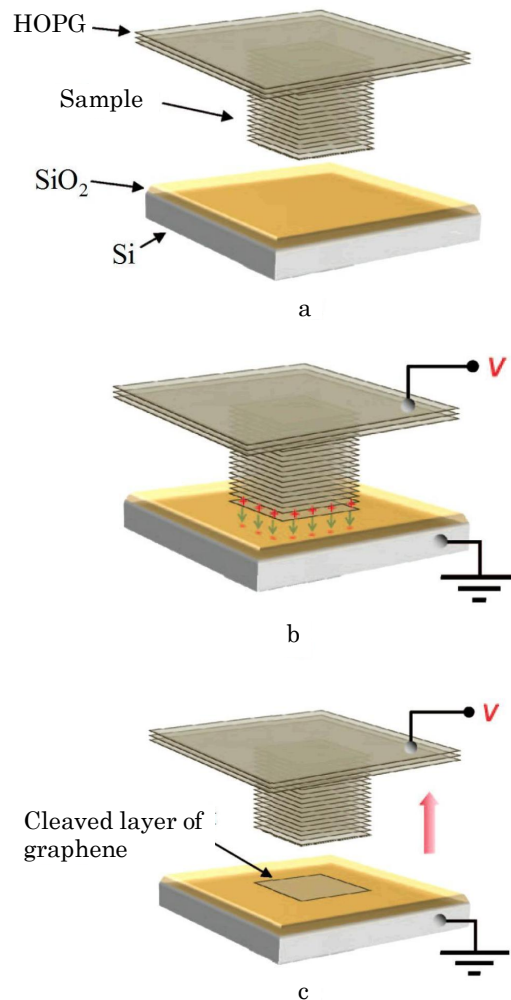


Fig. 10 – The scheme of exfoliation of graphite with deposited relief by electrostatic method: a) initial setup, in which relief structures are located on the HOPG sample; b) application of voltage between HOPG template and silicon substrate before the contact; c) exfoliation of graphite by electrostatic field during removal of HOPG sample from the substrate. (Reprinted with permission from [80]. Copyright [2009], American Chemical Society)

Thus, phenomenon of exfoliation of graphite plays an important role in both superlubricity and production of graphene. However, its theoretical investigation lags behind the level of the experimental data. Models of low friction of graphite are often based on the assumption about the presence of cleaved layers of graphene [5, 70, 81, 82]. Simulation of graphite nanoindentation by the classical MD [83-88] and boundary-element [89] methods has been performed. Diamond and virtual indenters [84, 85, 89] were applied for the study of mechanical characteristics of graphite [83, 84, 89] and formation of inter-laminar *sp*³ bonds at high pressures. However, repulsive forces between the indenter and sample in these works do not allow to exfoliate graphite mechanically (in contrast to the adhesive probes). Theoretical analysis of the HOPG exfoliation carried out in the work [80] is only aimed to the measurements of electric field, which is necessary for exfoliation, and does not clarify physics of the phenomenon.

Production of crystals of high structural and electronic quality is an indubitable advantage of the methods for producing graphene by exfoliation in connection with the absence in these crystals of a large number of defects. The presence in graphene of isolated point and linear defects is established by the method of scanning transmission electron microscopy (STEM) [90, 91]. Interaction of the crystal structure with ions and STEM electron beam leads to the lattice disturbance and appearance of point defects. Development of the graphene based devices requires knowledge of the formation conditions of defect structure there [76].

As known, nuclear fusion is accompanied by the process of graphite destruction by the plasma steam; therefore, investigation of defects in graphene and its failure at the bombardment of different particles is of interest for atomic power engineering [92, 93]. Action of plasma leads to the destruction of the graphite divertor in the experimental plants and thermonuclear reactors. A series of computer experiments based on the MD method [92-95] is devoted to the investigation of the given problem. Bombardment of graphene by single atoms of hydrogen isotopes and graphite irradiation by a stream of given particles are studied in the framework of new version of the Brenner potential and microcanonical statistical ensemble in the works [92, 93]. Particle energies and masses corresponding to the reflection, absorption and penetration into graphene, and also to the graphite fracture are determined. Consideration of the short-range Brenner potential, which describes the interaction between particles and carbon atoms, and single atoms (but not a beam of particles) for irradiation restricts the range of applicability of the results of numerical experiments [92, 93]. Moreover, the absence of accounting of heat dissipation in the specified systems influences the calculations. On the one hand, for example, in the two-dimensional model of a metal under the action of metallic atoms the energy of the latter can be transformed into the energy of defects formed in collisions [94]. On the other hand, small thickness of graphene leads to fast heat radiation to the environment [10]. In connection with this, further investigation of the stated problem is found to be urgent.

4. FRICTION OF METALLIC NANOPARTICLES

In spite of the fact that SFA and FFM allowed to significantly advance in the explanation of the atomistic nature of friction, the mentioned techniques are not without disadvantages [19, 21, and 96].

1. At present, FFM probes are made of silicon, silicon oxide and nitride, diamond (view of the sample can be arbitrary). Thus, there exists a rather limited spectrum of combinations of the studied materials. To extend the specified range, deposition of other materials on the FFM probe is used. However, as a rule, probes of poor quality and/or uncontrollable geometry are obtained in this case.

2. Amorphous or disordered tips of the FFM probes do not give the possibility to investigate the influence of ordered structures on friction that is necessary, for example, in the study of the superlubricity phenomenon.

3. In connection with the fixed radius of cantilever probes, investigation of the contact area in the range from tens of nm^2 for FFM to tens of thousands of μm^2

in SFA experiments is impossible. Moreover, for direct and independent measurement of the true contact area in FFM they often suggest certain geometry of the contact and a model of contact mechanics.

Consideration of friction of adsorbed nanoparticles (NP) at their shift by the AFM probe represents a new approach which allows one to avoid the stated disadvantages [96] (Fig. 11). A lot of experimental works [96-102] are devoted to the manipulation of nanoislands. In the majority of them only shift of NP is investigated and tribological properties of NP are not studied.

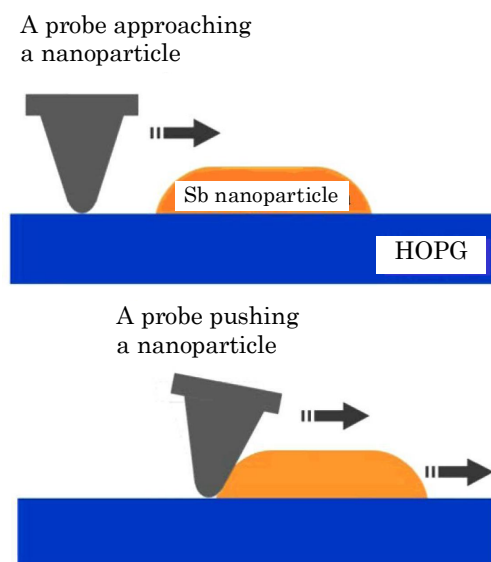


Fig. 11 – The scheme of the manipulation process. At the top: the AFM probe is scanning the surface in the contact mode and approaching a NP. At the bottom: the probe is shifting NP in the scanning direction. Additional bending of the probe is conditioned by the lateral force on the part of NP. (Reprinted with permission from [21],

<http://prb.aps.org/abstract/PRB/v82/i3/e035401>. Copyright [2010] by the American Physical Society)

Determination of the frictional properties of antimony NP adsorbed on HOPG and shifted by AFM probe in the ultrahigh (UH) vacuum is performed in the works [17, 19, 21, 96, 97, 103]. Areas of NP contact were in the range from 7000 to 200000 nm^2 . It was found that nanoislands with the contact area less than the order of 10^4 nm^2 are characterized by much smaller friction force than NP with larger areas. A linear dependence of the friction force on the contact area, where filled square markers correspond to the unoxidized ones due to UH nanoislands (Fig. 12), was discovered. A constant finite shear stress (black markers) or an insignificant friction (red markers) is observed. NP exposed to the environment before friction measurement are described by open symbols (triangles or circles). Triangles (grey) and circles (blue) correspond to the lines of finite and high values of the shear stresses, respectively. Slope of the linear branch formed by black symbols is approximately equal to 1.04 pN/nm^2 .

It is shown in the works [17, 19, 21] that some particles with areas larger than 10^4 nm^2 experience a very low friction, which is not even registered by the AFM; in this case other NP demonstrate a finite friction. This phenomenon was called “frictional duality”. The state

of low friction reminding a superlubricity has not yet obtained a sufficient explanation. It was primarily assumed [96, 103] that close to zero friction of small NPs is caused by their compact amorphous structure and incommensurability of the lattice of the NP surface and substrate. Here, the authors used the fact that in contrast to small nanoislands large NP are branched and their displacement as nonrigid objects is accompanied by additional energy dissipation. According to [17, 21], two friction states coexist due to the presence of impurities; and NP structure does not determine the frictional properties. Oxidation of the surfaces of some nano-clusters leads to friction growth by the order of magnitude. Since results of a part of the experiments, shown by triangles in Fig. 12, were not changed, it was concluded that the air influences not all NP in such a way. Additional investigation of crystalline incommensurable surfaces of gold NP on graphite has shown the non-linear scaling behavior of the friction force depending on the NP shape and orientation [97].

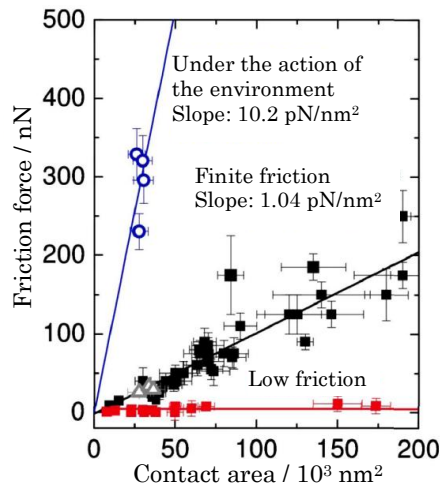


Fig. 12 – Friction force vs. the contact area of Sb NP moving on the HOPG substrate. (Reprinted with permission from [21], <http://prb.aps.org/abstract/PRB/v82/i3/e035401>. Copyright [2010] by the American Physical Society)

The absence of unambiguous interpretation of the experiments induced additional investigations including theoretical ones. Estimations of the experimentally observed values, given by analytical or semi-numerical approaches [96, 103, 104], are based on a number of assumptions and, in connection with this, do not allow to definitely explain the experiments. Numerical simulation of adsorbed metallic NP friction has not been performed until now. Ab initio investigation of the Sb NP properties on the HOPG surface [24] is inadequate in direct comparison of its results with the experimental ones because of the mismatch of time and spatial scales of the systems. MD method was used, mainly, for the study of diffusion of metallic nanoislands consisted of some hundreds of atoms on the graphite surface [105-107]. The specified computer experiments consider the ballistic friction of gold NP with velocities of about 100 m/s [108]. Here, calculation of the experimentally measured values is not performed; NP have small sizes as well as in [105-107], up to 3000 atoms. Experimentally observed NP sizes should, as minimum, 10 times exceed the noted values for the investigation of tribological characteristics.

As follows from the foregoing, further theoretical analysis of the friction of metallic NP on the graphite surface is required. In connection with fast development of new technologies of NP synthesis from different materials, for example, Ag [109, 110], Ni [111], Pt [112], it is necessary to extend the spectrum of radiated metals in the manipulation experiments.

Besides the context of tribology, interaction of NP with graphite structures and graphene is of direct importance for the production of new nanodevices. This is connected with the fact that influence of different nano-objects on graphene promotes the change of its electronic properties and structure [113-121].

5. CONCLUSIONS

In the given work we have presented a brief review of the experimental and theoretical investigation results of the tribological systems of some classes, namely, ultrathin liquid films, graphite systems and metallic NP.

Properties of the molecularly thin films confined in small spaces can be rather complex. They are determined by the structure of a liquid, structure and commensurability of surfaces, interaction potential between surface and liquid, load on walls, shear direction and rate. Unique properties of water, which have not obtained unambiguous explanation until now, conditioned importance of the investigation of tribological properties of an ultrathin film of water.

Hypothesis for the existence of a nanoflake attached to the FFM probe, which explains the superlubricity effect, requires the confirmation. In spite of the value of micromechanical cleavage of graphite for many production methods of graphene of high structural and electronic quality, there is deficiency of theoretical investigations of the realization conditions of this phenomenon. Knowledge of the latter can be useful for the production of graphene samples with the specified characteristics and development of new high-duty production techniques. Question about the influence of different factors, in particular, temperature on the exfoliation process remains still open. Since presence of defects in graphene considerably changes its electronic properties, explanation and discovery of the causes and conditions of defect formation in graphene is significant for the prediction of its characteristics [76].

Experimental investigations of friction of antimony NP on the HOPG surface allowed to discover the unique tribological properties, for example, superlubricity of NP. Understanding of the processes occurring at the contact of nano-objects with graphene is promising from the point of view of creation of new nanodevices.

ACKNOWLEDGEMENTS

The work has been performed under the financial support of the Ministry of Education and Science of Ukraine of the Project “Modeling of friction of metal nanoparticles and boundary liquid films which interact with atomically flat surfaces” (No 0112U001380) and training in Jülich Research Center by the invitation of Dr. Bo Persson.

REFERENCES

- B. Bhushan, J.N. Israelachvili, U. Landman, *Nature* **373**, 607 (1995).
- B.N.J. Persson, *Surf. Sci. Rep.* **33**, 83 (1999).
- B.N.J. Persson, *Sliding friction. Physical principles and applications* (Berlin: Springer-Verlag: 2000).
- B. Bhushan, *Nanotribology and nanomechanics* (Berlin: Springer-Verlag: 2005).
- M. Dienwiebel, *Atomic-scale friction and superlubricity studied using high-resolution frictional force microscopy: PhD, thesis* (The Netherlands: Leiden University: 2003).
- G.V. Dedkov, *Phys. Usp.* **43**, 541 (2000).
- O.M. Braun, A.G. Naumovets, *Surf. Sci. Rep.* **60**, 79 (2006).
- S. de Beer, M.H. Müser, *Soft Matter* **9**, 7234 (2013).
- K.L. Johnson, *Contact mechanics* (Cambridge: Cambridge University Press: 1985).
- R.P. Feynman, *Eng. Sci.* **23**, 22 (1960).
- B. Bhushan, *Springer handbook of nanotechnology* (Berlin: Springer-Verlag: 2003).
- A.D. Pogrebnjak, A.P. Shpak, V.M. Beresnev, D.A. Kolesnikov, Yu.A. Kunitzky, O.V. Sobol, V.V. Uglov, F.F. Komarov, A.P. Shpylyenko, A.A. Demyanenko, V.S. Baidak, V.V. Grudnitskii, *J. Nanosci. Nanotechnol.* **12**, 9213 (2012).
- A.D. Pogrebnjak, V.M. Beresnev, A.A. Demianenko, V.S. Baidak, F.F. Komarov, M.V. Kaverin, N.A. Makhmudov, D.A. Kolesnikov, *Phys. Solid State* **54**, 1882 (2012).
- B.N.J. Persson, *Surf. Sci. Rep.* **61**, 201 (2006).
- G. Binnig, C.F. Quate, Ch. Gerber, *Phys. Rev. Lett.* **56**, 930 (1986).
- C.M. Mate, G.M. McClelland, R. Erlandsson, S. Chiang, *Phys. Rev. Lett.* **59**, 1942 (1987).
- D. Dietzel, C. Ritter, T. Mönninghoff, H. Fuchs, A. Schirmeisen, U.D. Schwarz, *Phys. Rev. Lett.* **101**, 125505 (2008).
- D. Dietzel, M. Feldmann, H. Fuchs, U.D. Schwarz, A. Schirmeisen, *Appl. Phys. Lett.* **95**, 053104 (2009).
- A. Schirmeisen, U.D. Schwarz, *Chem. Phys. Chem.* **10**, 2373 (2009).
- G. Paolicelli, M. Rovatti, A. Vanossi, S. Valeri, *Appl. Phys. Lett.* **95**, 143121 (2009).
- D. Dietzel, T. Mönninghoff, C. Herding, M. Feldmann, H. Fuchs, B. Stegemann, C. Ritter, U.D. Schwarz, A. Schirmeisen, *Phys. Rev. B* **82**, 035401 (2010).
- D. Dietzel, M. Feldmann, C. Herding, U.D. Schwarz, A. Schirmeisen, *Tribol. Lett.* **39**, 273 (2010).
- M. Rovatti, G. Paolicelli, A. Vanossi, S. Valeri, *Meccanica* **46**, 597 (2011).
- J. Brndiar, R. Turanský, D. Dietzel, A. Schirmeisen, I. Stich, *Nanotechnology* **22**, 085704 (2011).
- A.D. Pogrebnjak, V.M. Beresnev, A.S. Kaverina, D.A. Kolesnikov, I.V. Yakushchenko, M.V. Ilyashenko, N.A. Makhmudov, *J. Frict. Wear* **33**, 195 (2012).
- M.L. Gee, P.M. McGuiggan, J.N. Israelachvili, A.M. Homola, *J. Chem. Phys.* **93**, 1895 (1990).
- J. Israelachvili, *Surf. Sci. Rep.* **14**, 109 (1992).
- J.N. Israelachvili, *Intermolecular and surface forces* (London: Academic Press: 1998).
- B.K. Yen, B.E. Schwickert, M.F. Toney, *Appl. Phys. Lett.* **84**, 4702 (2004).
- K.S. Novoselov, A.K. Geim, S.V. Morozov, D. Jiang, Y. Zhang, S.V. Dubonos, I.V. Grigorieva, A.A. Firsov, *Science* **306**, 666 (2004).
- A.K. Geim, *Science* **324**, 1530 (2009).
- C. Lee, X. Wei, Q. Li, R. Carpick, J.W. Kysar, J. Hone, *phys. status solidi b* **246**, 2562 (2009).
- C. Lee, Q. Li, W. Kalb, X.-Z. Liu, H. Berger, R.W. Carpick, J. Hone, *Science* **328**, 76 (2010).
- T. Filleter, J.L. McChesney, A. Bostwick, E. Rotenberg, K.V. Emtsev, Th. Seyller, K. Horn, R. Bennewitz, *Phys. Rev. Lett.* **102**, 86102 (2009).
- J. Ruan, B. Bhushan, *J. Appl. Phys.* **76**, 5022 (1994).
- J.M. Carlson, A.A. Batista, *Phys. Rev. E* **53**, 4153 (1996).
- V.L. Popov, *Tech. Phys.* **46**, 605 (2001).
- I.S. Aranson, L.S. Tsimring, V.M. Vinokur, *Phys. Rev. B* **65**, 125402 (2002).
- A.V. Khomenko, I.A. Lyashenko, *Condens. Matt. Phys.* **9**, 695 (2006).
- A.V. Khomenko, *Phys. Lett. A* **329**, 140 (2004).
- I.A. Lyashenko, A.V. Khomenko, L.S. Metlov, *Tribol. Int.* **44**, 476 (2011).
- A.E. Filippov, V.L. Popov, M. Urbakh, *Phys. Rev. Lett.* **106**, 025502 (2011).
- M.P. Allen, D.J. Tildesley, *Computer simulation of liquids* (Oxford: Clarendon Press: 1987).
- D. Frenkel, B. Smit, *Understanding molecular simulation* (London: Academic Press: 2002).
- D.C. Rapaport, *The art of molecular dynamics simulation* (Cambridge: Cambridge University Press: 2004).
- M. Griebel, S. Knapek, G. Zumbusch, *Numerical simulation in molecular dynamics* (Berlin: Heidelberg-Springer-Verlag: 2007).
- B. Bhushan, *Handbook of modern tribology* (Boca Raton: CRC Press: 2000).
- H. Yoshizawa, J. Israelachvili, *J. Phys. Chem.* **97**, 11300 (1993).
- J. Gao, W.D. Luedtke, U. Landman, *J. Chem. Phys.* **106**, 4309 (1997).
- J. Gao, W.D. Luedtke, U. Landman, *J. Phys. Chem. B* **101**, 4013 (1997).
- J. Gao, W.D. Luedtke, D. Gourdon, M. Ruths, J.N. Israelachvili, U. Landman, *J. Phys. Chem. B* **108**, 3410 (2004).
- A.V. Khomenko, N.V. Prodanov, *Condens. Matt. Phys.* **11**, 615 (2008).
- O.M. Braun, *Tribol. Lett.* **39**, 283 (2010).
- P.A. Thompson, G.S. Grest, M.O. Robbins, *Phys. Rev. Lett.* **68**, 3448 (1992).
- V.N. Samoilov, I.M. Sivebaek, B.N.J. Persson, *J. Chem. Phys.* **121**, 9639 (2004).
- P. Ball, *Chem. Rev.* **108**, 74 (2008).
- M.S.P. Sansom, I.D. Kerr, J. Breed, R. Sankararamakrishnan, *Biophys. J.* **70**, 693 (1996).
- P. Gallo, M.A. Ricci, M. Rovere, *J. Chem. Phys.* **116**, 342 (2002).
- P. Gallo, M. Rovere, *J. Phys.: Condens. Matt.* **15**, 7625 (2003).
- T. Patsahan, M. Holovko, *Condens. Matt. Phys.* **7**, 3 (2004).
- E. Spohr, A. Trokhymchuk, D. Henderson, *J. Electroanalytical Chem.* **450**, 281 (1998).
- L. Hua, X. Huang, R. Zhou, B.J. Berne, *J. Phys. Chem. B* **110**, 3704 (2006).
- C.D. Lorenz, M. Chandross, J.M.D. Lane, G.S. Grest, *Molecular Simul. Mater. Sci. Eng.* **18**, 034005 (2010).
- C.M. Mate, *IBM J. Res. Dev.* **39**, 617 (1995).
- J.A. Ruan, B. Bhushan, *J. Appl. Phys.* **76**, 8117 (1994).
- M.R. Falvo, J. Steele, R.M. II Taylor, R. Superfine, *Phys. Rev. B* **62**, 10665 (2000).
- H. Hölscher, D. Ebeling, U.D. Schwarz, *Phys. Rev. Lett.* **101**, 246105 (2008).
- C.M. Mate, *MRS Bull.* **27**, 967 (2002).
- M. Dienwiebel, G.S. Verhoeven, N. Pradeep, J.W.M. Frenken, J.A. Heimberg, H.W. Zandbergen, *Phys. Rev. Lett.* **92**, 126101 (2004).
- G.S. Verhoeven, M. Dienwiebel, J.W.M. Frenken, *Phys. Rev. B* **70**, 165418 (2004).
- A.K. Geim, K.S. Novoselov, *Nature Mater.* **6**, 183 (2007).
- A.H. Castro Neto, F. Guinea, N.M.R. Peres, K.S. Novoselov, A.K. Geim, *Rev. Mod. Phys.* **81**, 109 (2009).
- K.S. Novoselov, A.K. Geim, S.V. Morozov, D. Jiang, M.L. Katsnelson, I.V. Grigorieva, S.V. Dubonos, A.A. Firsov, *Nature* **438**, 197 (2005).
- S. Pisana, M. Lazzeri, C. Casiraghi, K. Novoselov, A.K. Geim, A.C. Ferrari, F. Mauri, *Nature Mater.* **6**, 198 (2007).

75. K.S. Novoselov, Z. Jiang, Y. Zhang, S.V. Morozov, H.L. Stormer, U. Zeitler, J.C. Maan, G.S. Boebinger, P. Kim, A.K. Geim, *Science* **315**, 1379 (2007).
76. H. Terrones, R. Lv, M. Terrones, M.S. Dresselhaus, *Rep. Prog. Phys.* **75**, 062501 (2012).
77. D.C. Elias, R.R. Nair, T.M.G. Mohiuddin, S.V. Morozov, P. Blanke, M.P. Halsall, A.C. Ferrari, D.W. Boukhvalov, M.I. Katsnelson, A.K. Geim, K.S. Novoselov, *Science* **323**, 610 (2009).
78. Y. Hernandez, V. Nicolosi, M. Lotya, F.M. Blighe, Z. Sun, S. De, I.T. McGovern, B. Holland, M. Byrne, Y.K. Gun'ko, J.J. Boland, P. Niraj, G. Duesberg, S. Krishnamurthy, R. Goodhue, J. Hutchison, V. Scardaci, A.C. Ferrari, J.N. Coleman, *Nature Nanotech.* **3**, 563 (2008).
79. W. Qian, R. Hao, Y. Hou, Y. Tian, C. Shen, H. Gao, X. Liang, *Nano Res.* **2**, 706 (2009).
80. X. Liang, A.S.P. Chang, Y. Zhang, B.D. Harteneck, H. Choo, D.L. Olynick, S. Cabrini, *Nano Lett.* **9**, 467 (2009).
81. A.E. Filippov, M. Dienwiebel, J.W.M. Frenken, J. Klafter, M. Urbakh, *Phys. Rev. Lett.* **100**, 046102 (2008).
82. K. Matsushita, H. Matsukawa, N. Sasaki, *Sol. State Comm.* **136**, 51 (2005).
83. O. Hod, *Chem. Phys. Chem.* **14**, 2376 (2013).
84. A. Richter, R. Ries, R. Smith, M. Henkel, B. Wolf, *Diam. Relat. Mater.* **9**, 170 (2000).
85. W. Guo, C.Z. Zhu, T.X. Yu, C.H. Woo, B. Zhang, Y.T. Dai, *Phys. Rev. Lett.* **93**, 245502 (2004).
86. A.V. Khomenko, N.V. Prodanov, *Carbon* **48**, 1234 (2010).
87. N.V. Prodanov, A.V. Khomenko, *Surf. Sci.* **604**, 730 (2010).
88. A.V. Khomenko, N.V. Prodanov, *J. Nano- Electron. Phys.* **3** No2, 34 (2011).
89. B. Yang, S. Mall, R.M. Rethinam, *J. Appl. Mech.* **76**, 011010 (2009).
90. M.H. Gass, U. Bangert, A.L. Bleloch, P. Wang, R.R. Nair, A.K. Geim, *Nature Nanotech.* **3**, 676 (2008).
91. F. Banhart, J. Kotakoski, A.V. Krasheninnikov, *ACS Nano.* **5**, 26 (2011).
92. H. Nakamura, A. Takayama, A. Ito, *Contrib. Plasma Phys.* **48**, 265 (2008).
93. A. Ito, H. Nakamura, *Thin Solid Films* **516**, 6553 (2008).
94. L.S. Metlov, *Phys. Rev. E.* **81**, 051121 (2010).
95. A.V. Khomenko, N.V. Prodanov, Yu.V. Scherbak, *J. Nano- Electron. Phys.* **1** No2, 66 (2009).
96. E. Gnecco, E. Meyer, *Fundamentals of friction and wear on the nanoscale* (Berlin: Springer-Verlag: 2007).
97. D. Dietzel, M. Feldmann, U.D. Schwarz, H. Fuchs, A. Schirmeisen, *Phys. Rev. Lett.* **111**, 235502 (2013).
98. R. Resch, A. Bugacov, C. Baur, B. Koel, A. Madhukar, A. Requicha, P. Will, *Appl. Phys. A.* **67**, 265 (1998).
99. C. Baur, A. Bugacov, B.E. Koel, A. Madhukar, N. Montoya, T.R. Ramachandran, A.A.G. Requicha, R. Resch, P. Will, *Nanotechnology* **9**, 360 (1998).
100. M. Martin, L. Roschier, P. Hakonen, U. Parts, M. Paalonen, B. Schleicher, E.I. Kauppinen, *Appl. Phys. Lett.* **73**, 1505 (1998).
101. M. Sitti, H. Hashimoto, *IEEE/ASME Trans. Mechatron.* **5**, 199 (2000).
102. A.D. Pogrebnjak, A.G. Ponomarev, A.P. Shpak, Yu.A. Kunitskii, *Phys. Usp.* **55**, 270 (2012).
103. C. Ritter, M. Heyde, B. Stegemann, K. Rademann, U.D. Schwarz, *Phys. Rev. B* **71**, 085405 (2005).
104. D.A. Aruliah, M.H. Müser, U.D. Schwarz, *Phys. Rev. B.* **71**, 085406 (2005).
105. W.D. Luedtke, U. Landman, *Phys. Rev. Lett.* **82**, 3835 (1999).
106. L.J. Lewis, P. Jensen, N. Combe, J.-L. Barrat, *Phys. Rev. B.* **61**, 16084 (2000).
107. B. Yoon, W.D. Luedtke, J. Gao, U. Landman, *J. Phys. Chem. B.* **107**, 5882 (2003).
108. R. Guerra, U. Tartaglino, A. Vanossi, E. Tosatti, *Nature Materials* **9**, 634 (2010).
109. S.-H. Jeon, P. Xu, N.H. Mack, L.Y. Chiang, L. Brown, H.-L. Wang, *J. Phys. Chem. C* **114**, 36 (2010).
110. R. Abargues, R. Gradess, J. Canet-Ferrer, *New J. Chem.* **33**, 913 (2009).
111. A. Geissler, M. He, J.-M. Benoit, P. Petit, *J. Phys. Chem. C.* **114**, 89 (2010).
112. C. Nethravathi, E.A. Anumol, M. Rajamathi, N. Ravishankar, *Nanoscale* **3**, 569 (2011).
113. Y. Shibuta, J.A. Elliott, *Chem. Phys. Lett.* **427**, 365 (2006).
114. M. Neek-Amal, R. Asgari, M.R. Rahimi Tabar, *Nanotechnology* **20**, 135602 (2009).
115. N. Patra, B. Wang, P. Král, *Nano Lett.* **9**, 3766 (2009).
116. V.H. Crespi, *Nature* **462**, 858 (2009).
117. M.I. Katsnelson, *Science.* **329**, 1157 (2010).
118. A.V. Khomenko, N.V. Prodanov, *J. Phys. Chem. C.* **114**, 19958 (2010).
119. A.V. Khomenko, N.V. Prodanov, B.N.J. Persson, *Condens. Matt. Phys.* **16**, 33401 (2013).
120. A.V. Khomenko, N.V. Prodanov, M.A. Khomenko, B.O. Krasyulya, *J. Nano- Electron. Phys.* **5**, 03018 (2013).
121. A. Vanossi, N. Manini, M. Urbakh, S. Zapperi, E. Tosatti, *Rev. Mod. Phys.* **85**, 529 (2013).